

# Entropic Image Thresholding Segmentation Based on Gabor Histogram

Sanli Yi, Guifang Zhang, Jianfeng He\*, Lirong Tong

School of Information Engineering and Automation, Kunming University of Science and Technology, Kunming  
650500, China

[e-mail: litch2004@sina.com, 1439402142@qq.com, 120112624@qq.com, 1183278950@qq.com]

\*Corresponding author: Jianfeng He

*Received June 28, 2018; revised October 3, 2018; accepted November 6, 2018;  
published April 30, 2019*

---

## **Abstract**

Image thresholding techniques introducing spatial information are widely used image segmentation. Some methods are used to calculate the optimal threshold by building a specific histogram with different parameters, such as gray value of pixel, average gray value and gradient-magnitude, etc. However, these methods still have some limitations. In this paper, an entropic thresholding method based on Gabor histogram (a new 2D histogram constructed by using Gabor filter) is applied to image segmentation, which can distinguish foreground/background, edge and noise of image effectively. Comparing with some methods, including 2D-KSW, GLSC-KSW, 2D-D-KSW and GLGM-KSW, the proposed method, tested on 10 realistic images for segmentation, presents a higher effectiveness and robustness.

---

**Keywords:** Image thresholding, Gabor histogram, spatial information;

## 1. Introduction

**I**mage segmentation is an important technique in image processing. It plays a critical role in computer vision, pattern recognition, medical image processing. A large number of image segmentation techniques have been developed so far, and the threshold segmentation is one of the most commonly used techniques due to its simplicity and ease of implementation.

A number of different kinds of thresholding methods have been reported, such as entropy thresholding [1], Otsu segmentation [2] and minimum error method [3], etc. Among these methods, the entropy thresholding proposed by Pun [4] is used to calculate the optimal threshold by maximizing the upper bound of a posteriori entropy. And many extensions based on Pun's method have been developed.

Entropic thresholding method based on 1D image histogram (KSW) is widely used, which does not consider the gray level spatial distribution information. To overcome this shortcoming, many different kinds of 2D histogram have been proposed by embedding spatial information. Abutaleb proposed to use the gray level of pixels as well as the average gray level of pixels in its neighborhood to construct 2D histogram (2D-KSW) [5]. Xiao used Gray-level Spatial Correlation (GLSC) to construct GLSC histogram (GLSC-KSW) [6]. Yimit proposed an entropic thresholding method based on 2-D direction (2D-D) histogram by using the local edge property computed from the orientation histogram of a gradient image (2D-D-KSW) [7]. These improved methods perform better than the method based on 1D histogram. However, they can not differentiate edge and noise pixels in image effectively. To solve this problem, Xiao proposed a new entropic thresholding algorithm (GLGM-KSW) [8] based on gray-level and gradient-magnitude histogram (GLGM histogram), which calculates the gray level occurrence probability and spatial distribution simultaneously. GLGM histogram possesses stronger capability for image components discrimination than 2D, GLSC and (2D-D) histogram. However, the anisotropic diffusion filtering is employed as the image preprocessing in constructing the GLGM histogram, the filtering operation thus has a negative effect on the recognition of image edges. Recently, the GLLV histogram constructed from gray level of pixels and the local variance of its neighboring was proposed by Xiulian Zeng [9]. Though the improved performance is obvious, 2D entropic thresholding methods still need enhance the performance of edge recognition.

As reviewed above, the histogram constructed by taking spatial information into account can improve the entropic thresholding performance. Image spatial information can be represented by its local texture features, and different texture features may distinguish foreground/background, edge and noise of image. Therefore, import of texture features to construct a histogram can improve edge recognition performance of the entropic thresholding. To develop a better technique for texture feature extraction, we propose the

entropic thresholding method based on Gabor histogram that a new 2D histogram (Gabor histogram) is constructed by Gabor filter simulating the receptive field of visual cortex, which can distinguish foreground/background, edge and noise of image effectively.

The remainder of this paper is organized as follows: in Section2 the proposed method is described. Then the experimental results are presented and compared with existing methods in Section3. Finally, conclusions are provided in Section4.

## 2. The proposed method

Embedding spatial information can improve the performance of entropic thresholding methods, while further work is still needed to improve the edge recognition performance. To solve this problem, a novel 2D Gabor histogram which can distinguish edge of image effectively is constructed, and the entropic thresholding method based on Gabor histogram is proposed. This method has briefly three steps, firstly Gabor filter is used to extract texture feature of image, and then Gabor histogram is constructed according to these texture feature, finally, the optimal entropy threshold based on the Gabor histogram is calculated.

### 2.1 Construction of Gabor histogram

The 2-D Gabor filter is a Gabor function constructed on structure information of image, which can well describe the local structure information corresponding to the spatial frequency (scale), spatial position and orientation selectivity [10]. Therefore, more accurate local structure information can be obtained through calculating its local optimal value. In this study, the Gabor histogram is constructed by using 2-D Gabor filter to indicate the gray scale, scale information and orientation information of image. In the following, we will introduce how to construct Gabor histogram.

For an image  $I(x, y)$  of size  $Q \times R$  with gray level set  $G = \{0, 1, \dots, 255\}$ , where  $x = 1, 2, \dots, Q$  and  $y = 1, 2, \dots, R$ . Firstly  $I(x, y)$  is convoluted with 2-D Gabor kernel function, defined as  $G(x, y)$ . And then a new image  $F(x, y)$  is obtained by:

$$F(x, y) = I(x, y) * G(x, y) \quad (1)$$

Where the \* means convolution operate.

A two-dimensional Gabor filter is a Gaussian kernel function modulated by a complex sinusoidal plane wave [11], defined as:

$$G(x, y) = \frac{f_{\alpha}^2}{\pi\gamma\eta} \exp\left(-\frac{x'^2}{\gamma^2} + \frac{y'^2}{\eta^2}\right) \exp(j2\pi f_{\alpha} x' + \phi) \quad (2)$$

$$x' = x \cos \theta_\beta + y \sin \theta_\beta$$

$$y' = -x \sin \theta_\beta + y \cos \theta_\beta$$

Where  $\gamma$  the sharpness along the major axis, and  $\eta$  the sharpness along the minor axis (perpendicular to the wave),  $\phi$  is the phase offset.  $f_\alpha$  is the frequency of the sinusoid,

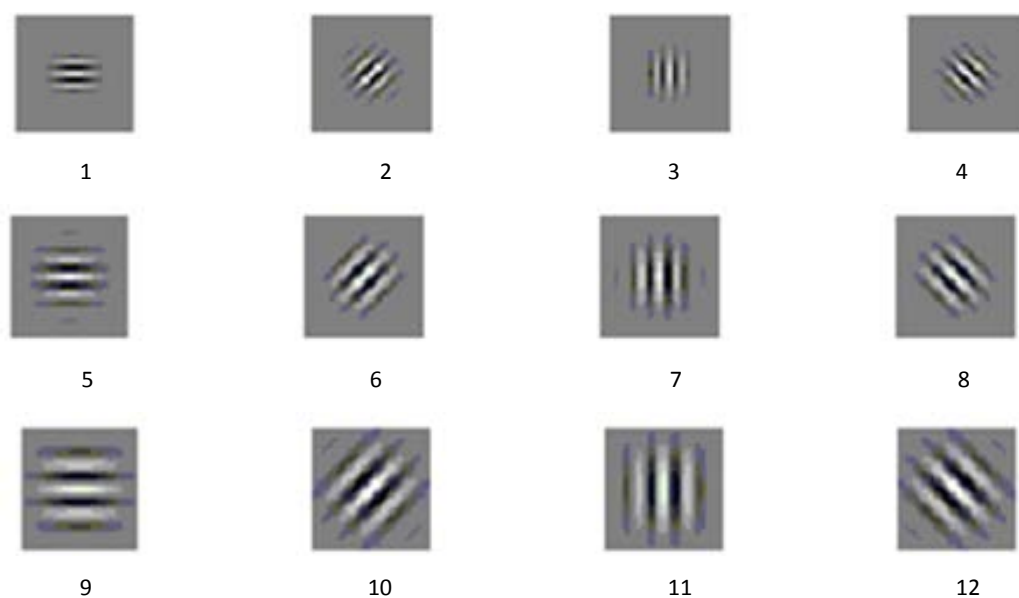
$$f_\alpha = \sqrt{2}^{-k1} f_{\max} \quad \alpha = \{0, \dots, n-1\}, \text{ where } f_{\max} \text{ is the maximum frequency of the sinusoid.}$$

$\theta_\beta$  represents the orientation of the normal to the parallel stripes of a Gabor function, and

$$\theta_\beta = \frac{\beta \cdot 2\pi}{m} \quad \beta \in \{0, \dots, m-1\}. \text{ The } n \text{ represents the number of scale and } m \text{ represents}$$

the number of direction. According to the numbers of scale and orientation,  $m \times n$  (instead as  $K$  in the fellow) 2-D Gabor kernel functions can be obtained.

In this paper, let the  $m$  be 4 and  $n$  be 5 (four orientations and five scales). The 4 orientations can basically display the main orientations of the texture details in image. The scale is selected from small to larger. And as too small scale can not reflect the image detail, and too large scale may make the calculation too complicated, 5 scales are selected. Thus 20 ( $4 \times 5 = 20$ ) Gabor filters in four orientations and five scales can be obtained, and they are shown in [Fig. 1](#).



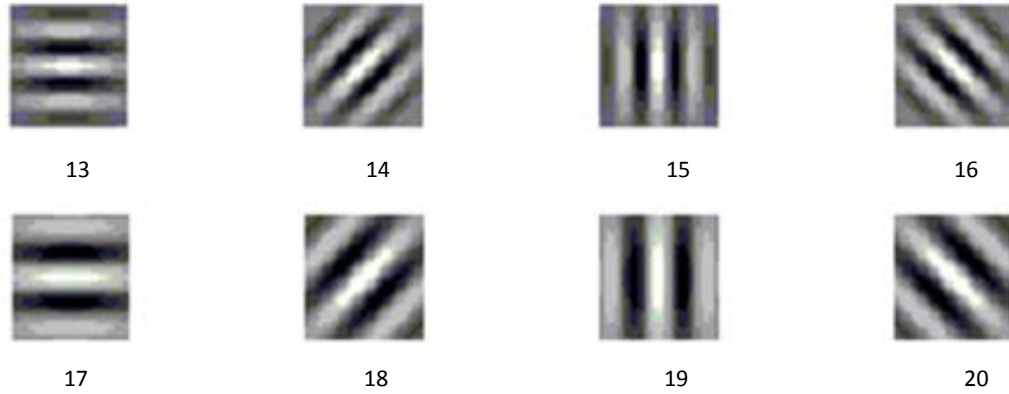


**Fig. 1.** Twenty Gabor filters with different directions and scales

Based on formula 1,  $I(x, y)$  is convoluted with twenty Gabor filters of different orientations and scales respectively, and then twenty convolution images  $F_K(x, y)$   $K \in \{1, 2, \dots, 20\}$  can be obtained. The filter is able to describe the detail edge information with the large neighborhood convolution value. Therefore, the maximum neighborhood convolution value is used to describe the edge information, defined as  $h_\Theta(x, y)$ :

$$h_\Theta(x, y) = \max\left(\sum_{j=-(w-1)/2}^{(w-1)/2} \sum_{i=-(w-1)/2}^{(w-1)/2} F_K(x+i, y+j)\right) \quad (3)$$

Let  $\Theta(x, y)$  represents the sign of convolution image with the maximum neighborhood convolution value  $h_\Theta(x, y)$ . Each pixel  $I(x, y)$  corresponding to an optimal Gabor filter, of which sign is  $\Theta(x, y)$ . The gray value of pixel  $I(x, y)$  and  $\Theta(x, y)$  can be used to construct Gabor histogram, calculated as:

$$h(s, q) = \text{prob}(f(x, y) = s \text{ and } \Theta(x, y) = q) \quad (4)$$

The normalized Gabor histogram is as follow:

$$\hat{h}(s, q) = \frac{\text{Num}(s, q)}{Q \times R} \quad (5)$$

$$\sum_{s=0}^{L-1} \sum_{t=1}^K \hat{h}(s, q) = 1 \quad (6)$$

Where  $s \in G$  and  $q \in \{1, 2, \dots, 20\}$ , the  $Num(s, q)$  represents the number of pixels with meeting the conditions of  $f(x, y) = s$  and  $\Theta(x, y) = q$ .  $Q \times R$  represents the number of pixels on whole image.

Take the Lena image as example, the Gabor histogram constructed by twenty Gabor filters is shown in Fig. 2.

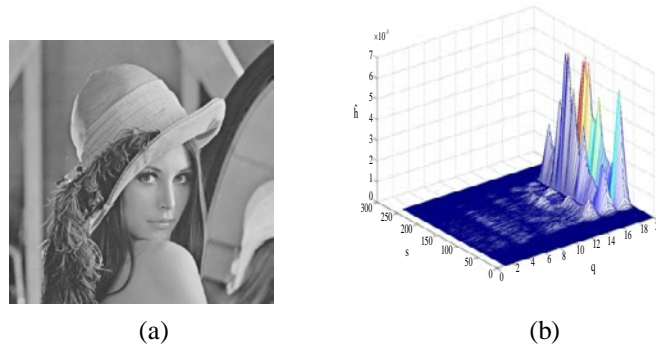


Fig. 2. Lena origin and its Gabor histogram: (a) Lena origin (b) Gabor histogram

## 2.2 Entropic threshold selection

Based on the Gabor histogram, the maximizing entropic criterion function is used to choose the optimal threshold. And the optimal threshold is computed as follows.

For an image  $I(x, y)$ , its gray level set  $G = \{0, 1, \dots, 255\}$ , and its probability function

$p(s, q)$  can be presented by the normalized Gabor histogram  $\hat{h}(s, q)$ :

$$p(s, q) = \hat{h}(s, q) \quad (7)$$

Where  $s \in G$  and  $q \in \{1, 2, \dots, 20\}$ .

Suppose that the pixels in the image are divided into two classes  $G_o = \{0, 1, 2, \dots, t\}$  and  $G_b = \{t+1, t+2, \dots, 255\}$  through a threshold  $t$ . Where  $G_o$  represents background and  $G_b$  is object or vice versa. And then the probability functions of two classes are given by:

$$\left[ \frac{p(0,1)}{P_o(t)}, \dots, \frac{p(0,K)}{P_o(t)}, \frac{p(1,1)}{P_o(t)}, \dots, \frac{p(t,K)}{P_o(t)} \right] \quad (8)$$

$$\left[ \frac{p(t+1,1)}{P_B(t)}, \dots, \frac{p(t+1,K)}{P_B(t)}, \frac{p(t+2,1)}{P_B(t)}, \dots, \frac{p(255,K)}{P_B(t)} \right] \quad (9)$$

Where  $P_O(t)$  and  $P_B(t)$  can be written as:

$$P_O(t) = \sum_{s=0}^t \sum_{q=1}^K p(s,q) \quad (10)$$

$$P_B(t) = \sum_{s=t+1}^{255} \sum_{q=1}^K p(s,q) \quad (11)$$

And:

$$P_O(t) + P_B(t) = 1 \quad (12)$$

The entropy of object and background are:

$$H_O(t) = - \sum_{s=0}^t \sum_{q=1}^K \frac{p(s,q)}{P_O(t)} \ln \left( \frac{p(s,q)}{P_O(t)} \right) \quad (13)$$

$$H_B(t) = - \sum_{s=t+1}^{255} \sum_{q=1}^K \frac{p(s,q)}{P_B(t)} \ln \left( \frac{p(s,q)}{P_B(t)} \right) \quad (14)$$

The entropy of whole image is:

$$\phi(t) = H_O(t) + H_B(t) \quad (15)$$

Finally, the optimal threshold  $t$  is selected by maximizing the  $\phi(t)$  shown as:

$$t^* = \arg \max \phi(t) \quad (16)$$

### 3. Experimental Results and Discussion

The proposed method is tested on various images to demonstrate its effectiveness and robustness. Ten images with different types of 1D histogram (including unimodal, bimodal and multimodal), contents and sizes are used. They are Brain ( $414 \times 360$ ), Cameraman ( $256 \times 256$ ), Airplane ( $512 \times 512$ ), Boat ( $512 \times 512$ ), Milkdrop ( $512 \times 512$ ), Woman ( $512 \times 512$ ), House ( $414 \times 360$ ), Money ( $500 \times 1192$ ), Lena ( $414 \times 360$ ), Goldhill ( $414 \times 360$ ), shown in Fig. 3. In order to further prove the effectiveness of the proposed method, Abutaleb's 2D-KSW [5], Xiao's GLSC-KSW [6], Yimit's 2D-D-KSW [7], Xiao's GLGM-KSW [8] are employed for comparison.



**Fig. 3.** Ten original images

### 3.1 Results

It is important to select appropriate parameters in experiment.  $K$  is the number of Gabor filter, its recommended value is 20 (same as  $m = 4$ ,  $n = 5$ ).  $W$  is the neighborhood size of maximum neighborhoods convolution operation, in this paper, different neighborhood size ( $3 \times 3$ 、 $5 \times 5$ 、 $7 \times 7$  and  $9 \times 9$ ) are tested on the images. The thresholds and segmentation images of the proposed method in different neighborhood size are shown in [Table 1](#) and [Fig. 4](#).

**Table 1.** The thresholds of the proposed method in different neighborhood size

Image	Size as 3x3	Size as 5x5	Size as 7x7	Size as 9x9
brian	54	54	54	54
cameraman	126	126	127	128
airplane	159	159	159	163
boat	106	106	106	106

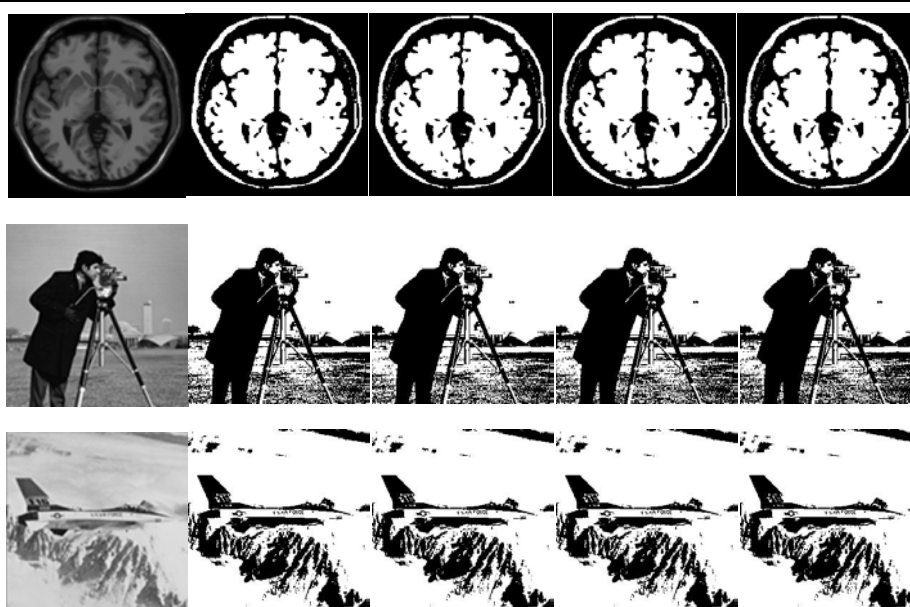




**Fig. 4.** Segmentation image of different neighborhood size, from left to right: original images,  $3 \times 3$ ,  $5 \times 5$ ,  $7 \times 7$  and  $9 \times 9$ .

As shown in **Fig. 4**, it can be observed that the segmentation results of different neighborhood size are similar. In this paper, the neighborhood size of  $7 \times 7$  is utilized to segment 10 images. And in order to demonstrate the effectiveness of the proposed method, the segmentation results of Abutaleb's 2D-KSW, Xiao's GLSC-KSW, Yimit's 2D-D-KSW, Xiao's GLGM-KSW and the proposed method are compared. The thresholds of different methods are shown in Table 2 and the segmentation images shown in **Fig. 4**.

**Table 2.** The threshold results of different approaches

Image	2D KSW	GLSC KSW	2D-D KSW	GLGM KSW	Our method
brian	56	65	68	54	54
cameraman	153	129	156	101	127
airplane	134	175	210	177	159
boat	60	126	148	116	106
milkdrop	80	84	90	33	124
woman	136	126	145	0	124
house	88	97	194	185	95
money	206	106	216	97	111
lena	127	113	141	111	129
goldhill	87	110	93	104	126

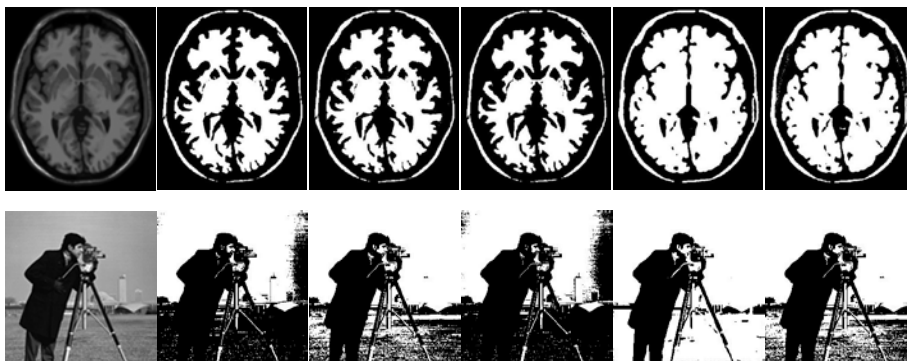




**Fig. 5.** Thresholding results of test images using different methods. From left to right: original images, the results obtained by 2D KSW, GLSC KSW, 2D-D KSW, GLGM KSW and our approach.

As shown in **Fig. 5** it can be observed that:

For Brain image, 2D KSW, GLSC KSW and 2D-D KSW can all split out the gray matter of the brain image, but these methods can not deal well with the dark information in image well. While GLGM-KSW and the proposed method can not only split out the gray matter, but also segment dark information.

For Cameraman and Money image, the 2D-D KSW and 2D KSW have a lot of black shadows effect which does not exist in the original image. While the GLSC KSW, GLGM KSW and the proposed method can yield better results.

For Airplane and Boat image, 2D-D KSW shows the black shadows. The results of other algorithms seem to be similar. While if we observe the segmentation result carefully, it can be found that the proposed method may indicate more details on the Boat image.

For Milkdrop image, only the proposed method can segment it effectively. Other approaches can not split well, especially GLGM KSW, which can not distinguish the background and drop of milk.

For Woman image, all the methods except GLGM KSW can get good result.

For House image, GLGM KSW and 2D-D KSW can only extract the contour of target, but can not handle the details in the image well. While 2D KSW, GLSC KSW and the proposed method can distinguish different image components effectively, and get satisfied results.

For Lena image, only 2D-D KSW shows some black shadows, other approaches have better similar segmentation results without black shadows.

For Goldhill image, all approaches show similar results. However, the results of the proposed method and GLSC KSW present better details in the sky of the image.

From the above experiment, we can see that, the proposed method may comprehensively reach good segmentation results.

### 3.2 Discussion

To quantitatively judge the quality of several thresholding-based segmentation algorithms, the uniformity measure [12] and the feature similarity [13] are used to further quantify the experimental results of different segmentation methods.

The uniformity measure may have a good judgment on the quality of the threshold image in the region consistency. It is extensively utilized in a lot of literatures and is given as:

$$u = 1 - 2 * p * \frac{\sum_{j=0}^p \sum_{i \in R_j} (f_i - u_j)^2}{N * (f_{\max} - f_{\min})} \quad (17)$$

Where  $N$  is the number of image pixels,  $p$  is number of threshold,  $f_i$  is the gray level of pixel  $i$ ,  $R_j$  represents  $j$ th segmented region,  $u_j$  is the mean gray value of the pixels in  $j$ th region,  $f_{\max}$  is the maximum gray level of pixels in the given image,  $f_{\min}$  is the minimum gray level of pixels in the given image. The uniformity measure  $u$  has a range in

[0, 1]. The value of  $u$  is closer to 1, that indicates the better uniformity in the segmented image and the better segmentation result is.

Feature similarity [14] is used to calculate the similarity of two images from the visual features of texture, shape and space position. The concrete formula is as follow:

$$FSIM = \frac{\sum_{X \in \Omega} S_L(X) PC_m(X)}{\sum_{X \in \Omega} PC_m(X)} \quad (18)$$

Where

$$\begin{aligned} S_L(X) &= S_{PC}(X) S_G(X); \\ S_{PC}(X) &= \frac{2PC_1(X)PC_2(X) + T_1}{PC_1^2(X) + PC_2^2(X) + T_1}; \\ S_G &= \frac{2G_1(X)G_2(X) + T_2}{G_1^2(X) + G_2^2(X) + T_2} \end{aligned} \quad (19)$$

The  $\Omega$  in Eq 18 represents the whole space of image. T1 and T2 are constants. Here,  $T_1=0.85$ ,  $T_2=160$  [13].  $G$  represents the gradient of image, defined as below:

$$G = \sqrt{G_x^2 + G_y^2} \quad (20)$$

PC represents phase consistency, defined as below:

$$PC(X) = \frac{E(X)}{(\varepsilon + \sum nA_n(X))} \quad (21)$$

Where the  $A_n(X)$  represents  $n$  order amplitude,  $E(X)$  represents  $n$  order response vector level at position  $X$ .  $\varepsilon$  is a small positive constant. The higher the value of feature similarity means the better the segmentation result.

**Table 3** and **Table 4** show the uniformity measure and the feature similarity of different methods respectively.  $\bar{\omega}_1$  and  $\bar{\omega}_2$  represent the average uniformity measure and feature similarity.

**Table 3.** Uniformity measure of different methods

Image	2D-KSW	GLSC KSW	2D-D KSW	GLGM KSW	Our method
brian	0.9842	0.9846	0.9836	<b>0.9879</b>	<b>0.9879</b>
cameraman	0.9403	0.9651	0.9358	<b>0.9796</b>	0.9668
airplane	0.9821	0.9814	0.9278	0.9807	<b>0.9844</b>
boat	0.9753	0.9795	0.9635	0.9821	<b>0.9828</b>
milkdrop	0.9476	0.9490	0.9509	0.9238	<b>0.9637</b>
woman	0.9754	<b>0.9771</b>	0.9713	0.9205	<b>0.9771</b>

house	0.9629	0.9679	0.9502	<b>0.9811</b>	0.9663
money	0.9155	0.9605	0.8893	0.9557	<b>0.9625</b>
lena	0.9825	0.9809	0.9805	0.9804	<b>0.9825</b>
goldhill	0.9522	0.9621	0.9555	0.9603	<b>0.9648</b>
$\bar{\omega}_1$	0.9618	0.9708	0.9508	0.9652	<b>0.9738</b>

**Table 4.** Feature similarity of different methods

Image	2D KSW	GLSC KSW	2D-D KSW	GLGM KSW	Our method
brain	0.6406	0.6397	0.6439	<b>0.6629</b>	0.6556
cameraman	0.6463	0.6596	0.6390	<b>0.7173</b>	0.6620
airplane	0.7012	0.6902	0.4592	0.6763	<b>0.7118</b>
boat	0.5648	0.6014	0.5086	0.5984	<b>0.6275</b>
milkdrop	0.6523	0.6405	0.6244	0.6323	<b>0.6570</b>
woman	0.5881	0.6094	0.5636	0	<b>0.6111</b>
house	0.7838	0.7914	0.6378	0.7427	<b>0.7933</b>
money	0.5152	0.7477	0.3970	0.6884	<b>0.7497</b>
lena	0.65895	0.63898	0.6332	0.63383	<b>0.6585</b>
goldhill	0.5514	0.5625	0.5611	0.5460	<b>0.5664</b>
$\bar{\omega}_2$	0.6014	0.6581	0.5668	0.5898	<b>0.6693</b>

According to [Table 3](#) and [Table 4](#), we can find some clues:

For Milkdrop image, other methods may not split it well, while only the proposed approach presents a better result, which means Gabor histogram having an advantage over the images that the contour information is not very obvious.

For House image, GLGM-KSW shows the best uniformity measure value, while the proposed method indicates the best feature similarity. This result is reasonable, because the evaluation of the degree of uniformity measurement and feature similarity are the different aspects of the evaluation. Uniformity measure focuses on the consistency of the threshold, and the feature similarity is committed to the texture, shape and spatial location and other visual features to evaluate the quality of image.

GLGM-KSW presents a better result on Brain and Cameraman. However, this method relies too much on the contour information of the image. Once the contour information is not very obvious, the segmentation result is not well, such as the results of Milkdrop and Woman images.

In most cases, 2D-D-KSW relatively shows poor segmentation results. It has a worst uniformity measure value (0.9508) and feature similarity value (0.5668) for the images,

because it does not use the simple gradient direction information to distinguish the different information of the image. GLSC-KSW performs better than 2D-KSW, because the GLSC histogram stresses the edge information, while 2D histogram ignores the side of the diagonal information, which may lose some useful information.

The proposed method exhibits better results in most cases. In addition, it reveals the best average value of uniformity measure (0.9738) and feature similarity (0.6693), which indicates the proposed has a better effectiveness and robustness.

## 4. Conclusion

In this paper, a new Gabor histogram is constructed by including the spatial frequency domain information and spatial location information, and the entropic thresholding method based on Gabor histogram is proposed, which can effectively distinguish foreground/background, edge and noise of image. In experiment, 10 images with different histogram types are used to demonstrate the performance of the proposed method. The evaluation of visualized and qualitative results shows that the proposed method, compared with other methods, can achieve better results.

## Reference

- [1] F. Nie, P. Zhang, J. Li, et al, "A novel generalized entropy and its application in image thresholding," *Signal Processing*, vol. 134, no. C, pp. 23-34, 2017. [Article \(CrossRefLink\)](#).
- [2] N. Otsu, "Threshold Selection Method from Gray-Level Histograms," *Systems Man and Cybernetics IEEE Transactions on*, vol. 9, no. 1, pp. 62-66, 1979. [Article \(CrossRefLink\)](#).
- [3] J. Kittler and J. Illingworth, "Minimum error thresholding," *Pattern Recognition*, vol. 19, no. 1, pp. 41-47, 1986. [Article \(CrossRefLink\)](#).
- [4] T. Pun, "Entropic thresholding, a new approach," *Computer Graphics and Image Processing*, vol. 16, no. 3, pp. 210-239, 1981. [Article \(CrossRefLink\)](#).
- [5] Abutaleb A S, et al, "Automatic thresholding of gray-level pictures using two-dimensional entropy," *Compute Vision Graphics and Image Processing*, vol. 47, no. 1, pp. 22-32, 1989. [Article \(CrossRefLink\)](#).
- [6] Y. Xiao, Z. Cao and S. Zhong, "New entropic thresholding approach using gray-level spatial correlation histogram," *Optical Engineering*, vol. 49, no. 12, pp. 1127-1134, 2010. [Article \(CrossRefLink\)](#).
- [7] A.Yimit, Y. Hagihara, T. Miyoshi and Y. Hagihara, "2-D direction histogram based entropic thresholding," *Neuro computing*, vol. 120, no. 10, pp. 287-297, 2013. [Article \(CrossRefLink\)](#).
- [8] Y. Xiao, Z. Cao and S. Zhong, "Entropic image Thresholding Based on GLGM Histogram," *Pattern Recognition Letters*, vol. 40, no. 1, pp. 47-55, 2014. [Article \(CrossRefLink\)](#).
- [9] X. Zheng, H. Ye and Y. Tang, "Image Bi-Level Thresholding Based on Gray Level-Local Variance Histogram," *Entropy*, vol. 19, no. 5, pp. 191, 2017. [Article \(CrossRefLink\)](#).

- [10] Y. D. Zhao, L. P. Zhang and P. X. Li, "A Texture Segmentation Algorithm Based on Directional Gabor Filter," *Journal of Image and Graphics*, vol. 11, no. 4, pp. 504-510, 2006. [Article \(CrossRefLink\)](#).
- [11] M. Haghighat, S. Zonouz and M.A. Mottaleb, "CloudID: Trustworthy cloud-based and cross-enterprise biometric identification," *Expert Systems with Applications*, vol. 42, no. 21, pp. 7905–7916, 2015. [Article \(CrossRefLink\)](#).
- [12] S. Manikanda, K. Ramar, M. W. Iruthayarajan, et al, "Multilevel thresholding for segmentation of medical brain images using real coded genetic algorithm," *Measurement*, vol. 47, no. 1, pp. 558-568, 2014. [Article \(CrossRefLink\)](#).
- [13] A. K. Bhandari and K. S. Vineet, "Cuckoo search algorithm and wind driven optimization based study of satellite image segmentation for multilevel thresholding using Kapur's entropy," *Expert Systems with Applications*, vol. 41, no. 7, pp. 3538-3560, 2014. [Article \(CrossRefLink\)](#).
- [14] Z. Lin, Z. Lei, et al, "FSIM: A feature similarity index for image quality assessment," *IEEE Transactions on Image Processing*, vol. 20, no. 8, pp. 2378–2386, 2011. [Article \(CrossRefLink\)](#).



**Sanli Yi** (1977-), female, she is currently a lecturer in School of Information Engineering and Automation, Kunming University of Science and Technology.

Research area: Digital Image Processing.

E-mail: litch2004@sina.com



**Guifang Zhang** (1993-), female, she is currently a postgraduate student in School of Information Engineering and Automation, Kunming University of Science and Technology.

Research area: Digital Image Processing.

E-mail: 1439402142@qq.com



**Jianfeng He** (1965-), male, he is currently a professor in School of Information Engineering and Automation, Kunming University of Science and Technology.

Research area: Digital Image Processing

E-mail: 120112624@qq.com



**Lirong Tong** (1993-), female, she is currently a postgraduate student in School of Information Engineering and Automation, Kunming University of Science and Technology.

Research area: Digital Image Processing.

E-mail: 1183278950@qq.com